University of California
Lawrence Livermore
National Laboratory

GEMINI
8-M Telescopes
Project

Beam Transfer Optics
Preliminary Design Report

Gemini North and South LGS AO
Preliminary Design Review Material

Prepared By: Brian Bauman and Don Gavel

Lawrence Livermore National Laboratory

Compiled by: Céline d'Orgeville, Gemini

April 26, 2001

Version: Draft

Revision Control

1. BTO components detailed designs

1.1. Relay telescope design

The design below gives an initial design for a relay telescope. The design assumes a total length between the PA and FSA of 20m, an interbeam spacing of 27mm, and 5 beams aligned above one another at the FSA. The result is a 1:1 afocal telescope with pupils at the front and rear focal points of the two lenses (i.e., a "4f system"). Note that this model should not be used to assess image quality of each beam since the incoming light is not collimated; this approach was chosen for simplicity. This model is useful for sizing lens apertures; it models the chief rays correctly. Not surprisingly, when modeled to evaluate image quality, the very slow optics and small beams yield <<λ/100 P-V wavefront quality for the nominal design.

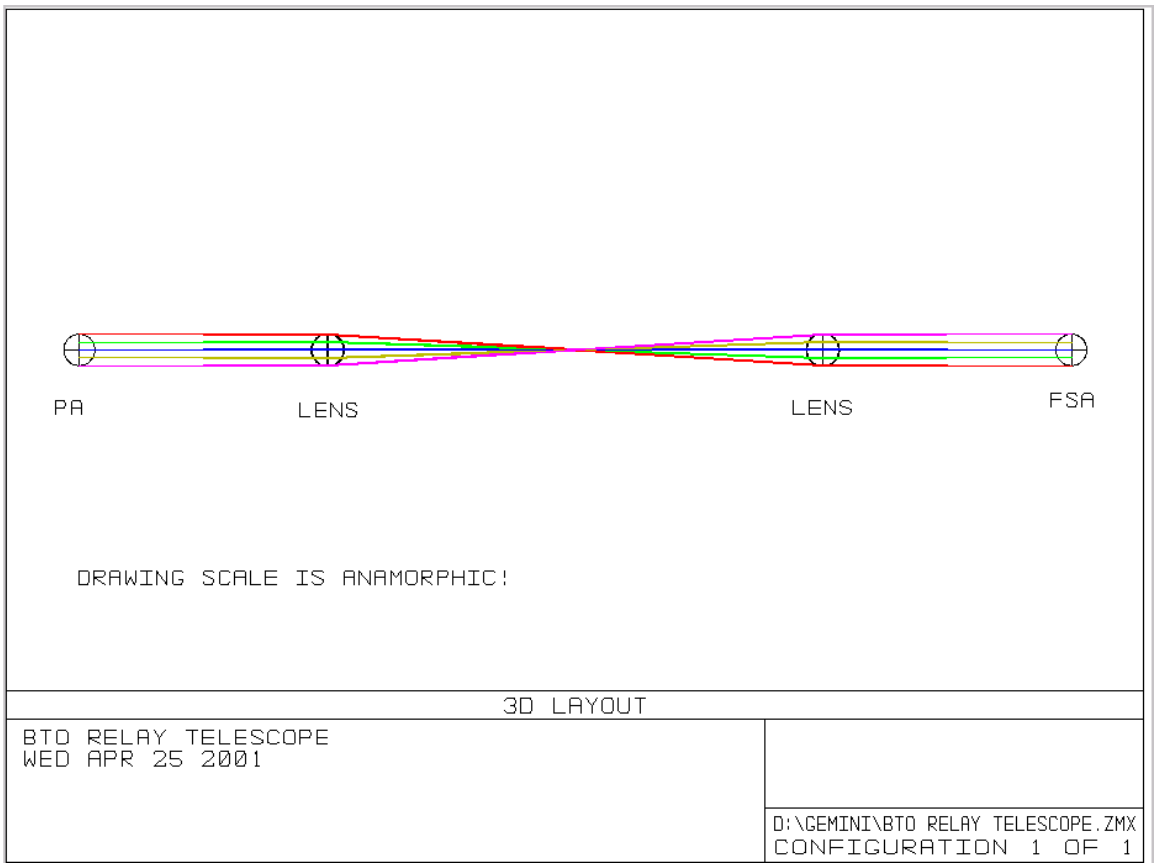

Lens Data Editor

Edit Solves Options Help

Surf:Type		Comment	Radius		Thickness		Glass		Semi-Diameter		Conic
OBJ	Standard	POINTING ARRAY	Infinity		0.000000				55.000000		0.000000
1	Standard		Infinity		5000.000000				55.000000		0.000000
2	Standard	LENS, F=5M	2292.066025	X	20.000000		SILICA		57.385209		0.000000
3	Standard		Infinity		4975.819798	V			57.239741		0.000000
STO	Standard		Infinity		-4975.819798	P			2.500000	U	0.000000
5	Standard		Infinity		9962.106280				57.239741		0.000000
6	Standard	LENS, F=5M	Infinity		20.000000		SILICA		57.368835		0.000000
7	Standard		-2292.066025	X	5000.000000	M			57.514267		0.000000
IMA	Standard	FAST STEERING ARRAY	Infinity						55.004400		0.000000

Title: BTO relay telescope
Date : WED APR 25 2001

LENS NOTES:

relays plane near laser source (pointing array) to fast steering mirror array (FSA)
modelled as 1:1 afocal telescope with object/image at PA/FSA and telecentric pupil; correctly describes chief rays for purposes of optics sizing
5 beams in vertical arrangement modelled, with 27.5mm between adjoining beams at the FSA

GENERAL LENS DATA:

Surfaces	:	8
Stop	:	4
System Aperture	:	Float By Stop Size = 2.5
Glass Catalogs	:	Schott MISC
Ray Aiming	:	Off
Apodization	:	Uniform, factor = 0.00000E+000
Effective Focal Length	:	2388539 (in air)
Effective Focal Length	:	2388539 (in image space)
Back Focal Length	:	-2383539
Total Track	:	20002.11
Image Space F/#	:	1000.002
Paraxial Working F/#	:	1000
Working F/#	:	1000
Image Space NA	:	0.0004999999
Object Space NA	:	0.0004999999
Stop Radius	:	2.5
Paraxial Image Height	:	55
Paraxial Magnification	:	-1
Entrance Pupil Diameter	:	2388.535
Entrance Pupil Position	:	2388535
Exit Pupil Diameter	:	1e+007
Exit Pupil Position	:	1e+010
Field Type	:	Object height in Millimeters
Maximum Field	:	55
Primary Wave	:	0.589
Lens Units	:	Millimeters
Angular Magnification	:	-1.627686e-006

Fields : 5
Field Type: Object height in Millimeters

#	X-Value	Y-Value	Weight
1	0.000000	0.000000	4.000000
2	0.000000	27.500000	1.000000
3	0.000000	55.000000	1.000000
4	0.000000	-27.500000	1.000000
5	0.000000	-55.000000	1.000000

Vignetting Factors

#	VDX	VDY	VCX	VCY	VAN
1	0.000000	0.000000	0.000000	0.000000	0.000000
2	0.000000	0.000000	0.000000	0.000000	0.000000
3	0.000000	0.000000	0.000000	0.000000	0.000000
4	0.000000	0.000000	0.000000	0.000000	0.000000
5	0.000000	0.000000	0.000000	0.000000	0.000000

Wavelengths : 1
Units: Microns

#	Value	Weight
1	0.589000	1.000000

SOLVE AND VARIABLE DATA:

Curvature of 2 : Solve, power = 0.00020
Thickness of 3 : Variable
Thickness of 4 : Solve, pick up value from 3, scaled by -1.00000, plus 0.00000
Semi Diameter 4 : Fixed
Curvature of 7 : Solve, power = 0.00020
Thickness of 7 : Solve, marginal ray height = 0.00000

1.2. Details of diagnostics design

The diagnostics package, consisting of a centering diagnostic and a pointing diagnostic, must be designed so that their respective fields are large enough to capture an initial, roughly-aligned system, yet with enough resolution to operate in closed-loop.

1.2.1. Pointing diagnostic

The pointing diagnostic, which images the far-field, certainly must have a FOV larger than the size of the constellation (85 arcsec across on the sky=24 mrad in BTO space) for closed-loop operation plus initial alignment errors (approximately 80 arcsec on the sky=23 mrad in BTO space), for a total of about 165 arcsec=47 mrad in BTO space. This is consistent with a FOV large enough to boresight the LLT to the main telescope during LLT installation, accomplished by looking at a natural star with the pointing diagnostic and the telescope guider camera.

The candidate CCD (Cooke Corp. Pixelfly SVGA, 1280x1024, 6.7 micron square pixels) has at least 1000 pixels across each dimension, so a FOV of 165 arcsec would yield a pixel size of 0.165 arcsec. Thus, the typical pointing spot may be 2 or 3 pixels across in open t/t loop mode, and will broaden to perhaps 6 pixels in closed t/t loop mode (the spot broadens because the diagnostic is downstream of the fast t/t mirror, which is steering according to the atmospheric seeing). This is a configuration more than accurate enough to allow the fast t/t system to "capture".

This plate scale of 0.165 arcsec/pixel is accomplished by placing the camera at the focus of a 143mm lens. A 150mm focal length lens (Linos #038909) was selected for this initial design. The performance of this lens is diffraction-limited throughout the field, and is particularly good within the field of the constellation. Thus the pointing sensor can be used as an indicator of beam quality entering the LLT. The aperture of the lens clips part of the extreme edge of the field (see layout and footprint diagram), but this is unimportant for acquisition purposes.

The footprint diagram also suggests the configuration of the chopper wheel that selects the various beams for viewing. Since the 5 beams are well-separated in the plane just in front of the pointing lens (which is near the entrance of the diagnostics package), this is a natural place to position a chopper wheel.

Note that for rough boresighting of the LLT to the main telescope, it may be desirable to replace this lens with a shorter focal length lens.

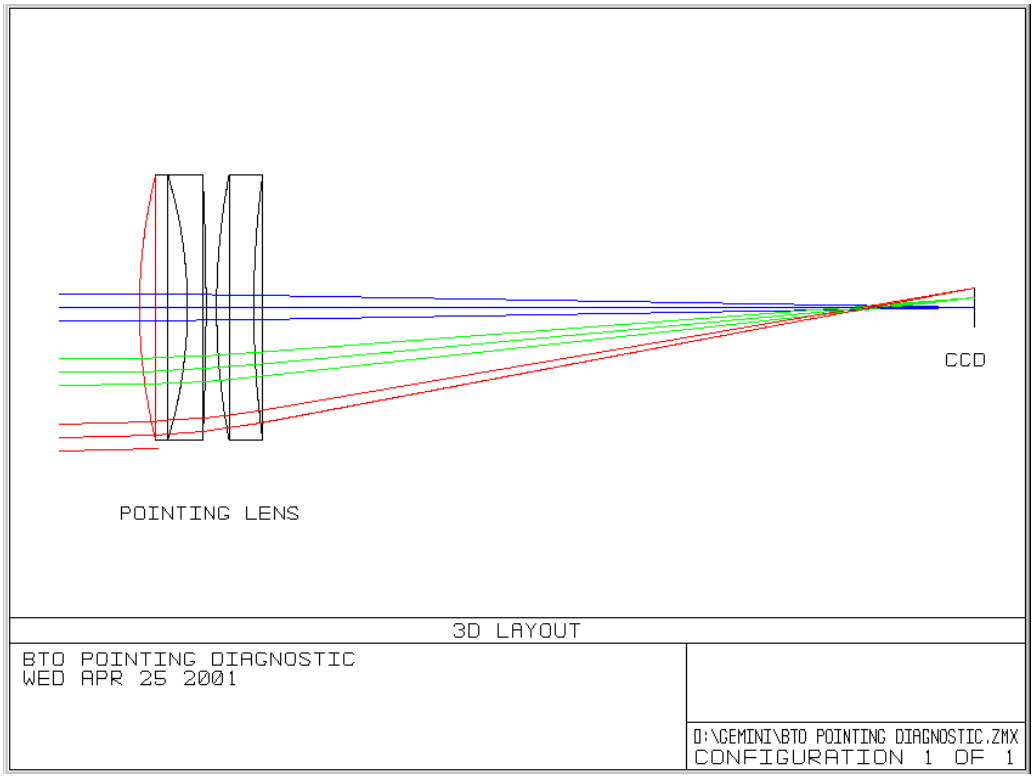
CCD
POINTING LENS
3D LAYOUT
BTO POINTING DIAGNOSTIC
WED APR 25 2001
D:\GEMINI\BTO POINTING DIAGNOSTIC.ZMX
CONFIGURATION 1 OF 1

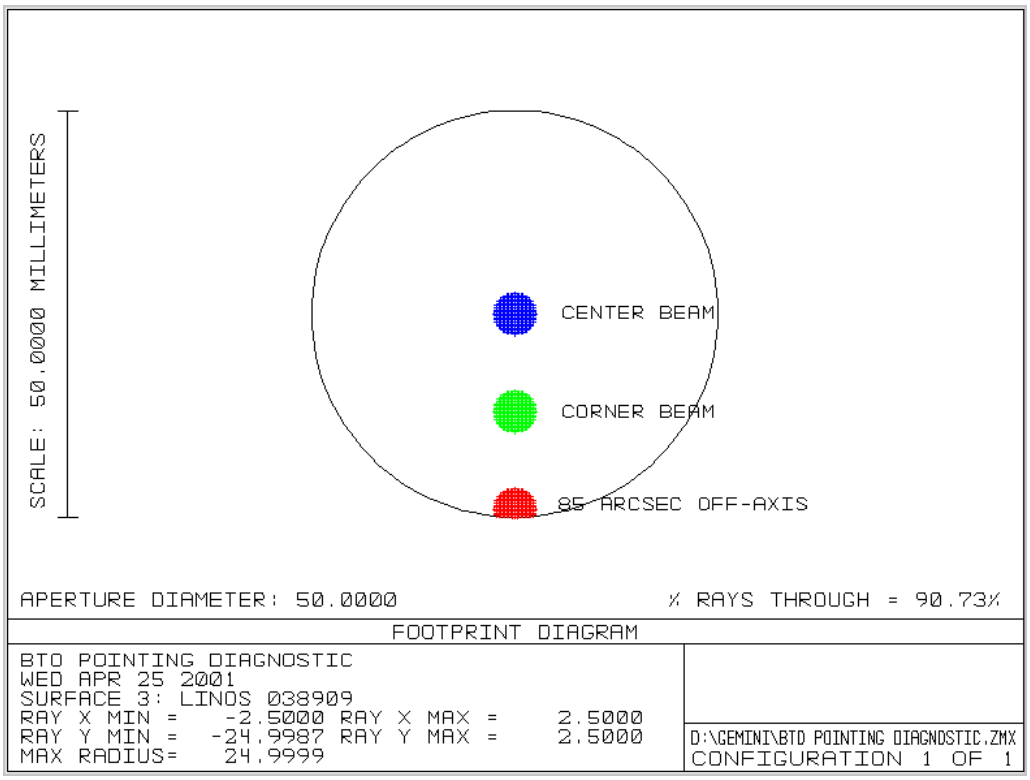
SCALE: 50.0000 MILLIMETERS
CENTER BEAM
CORNER BEAM
85 ARCSEC OFF-AXIS
APERTURE DIAMETER: 50.0000
% RAYS THROUGH = 90.73%
FOOTPRINT DIAGRAM
BTO POINTING DIAGNOSTIC
WED APR 25 2001
SURFACE 3: LINOS 038909
RAY X MIN = -2.5000 RAY X MAX = 2.5000
RAY Y MIN = -24.9987 RAY Y MAX = 2.5000
MAX RADIUS= 24.9999
D:\GEMINI\BTO POINTING DIAGNOSTIC.ZMX
CONFIGURATION 1 OF 1

Lens Data Editor

Edit Solves Options Help

Surf:Type		Comment	Radius	Thickness		Glass		Semi-Diameter		Conic
OBJ	Standard		Infinity	Infinity				Infinity		0.000000
STO	Standard	LLT ENTRANCE PUPIL	Infinity	-1000.000000				2.500000		0.000000
2	Standard		Infinity	15.000000				0.000000	U	0.000000
3*	Standard	LINOS 038909	104.405930	9.000000		BK7		25.000000	U	0.000000
4*	Standard		-86.595081	3.500000		F2		25.000000	U	0.000000
5*	Standard		-508.388409	2.000000				25.000000	U	0.000000
6*	Standard		133.351113	7.000000		SF11		25.000000	U	0.000000
7*	Standard		185.666543	135.560867	M			25.000000	U	0.000000
8	Standard		Infinity	-0.017155				3.654837		0.000000
IMA	Standard	CCD	Infinity					3.651905		0.000000

```
System/Prescription Data

File : D:\Gemini\BTO pointing diagnostic.ZMX
Title: BTO pointing diagnostic
Date : WED APR 25 2001

LENS NOTES:

       uses Cooke Corp. Pixelfly SVGA camera



GENERAL LENS DATA:

Surfaces                 :                9
Stop                     :                1
System Aperture          : Entrance Pupil Diameter = 5
Glass Catalogs           : Schott
Ray Aiming               : Off
Apodization              :Uniform, factor =   0.00000E+000
Effective Focal Length   :        148.7977 (in air)
Effective Focal Length   :        148.7977 (in image space)
Back Focal Length        :        135.5609
Total Track              :            1000
Image Space F/#          :        29.75954
Paraxial Working F/#     :        29.75954
Working F/#              :        29.75898
Image Space NA           :      0.01679897
Object Space NA          :        2.5e-010
Stop Radius              :             2.5
Paraxial Image Height    :        3.636537
Paraxial Magnification   :               0
Entrance Pupil Diameter  :               5
Entrance Pupil Position  :               0
Exit Pupil Diameter      :       0.6565383
Exit Pupil Position      :       -19.52112
Field Type               : Angle in degrees
Maximum Field            :             1.4
Primary Wave             :           0.589
Lens Units               :   Millimeters
Angular Magnification    :        7.615702

Fields          : 3
Field Type: Angle in degrees
#         X-Value         Y-Value          Weight
 1        0.000000        0.000000        4.000000
 2        0.000000        0.700000        1.000000
 3        0.000000        1.400000        1.000000

Vignetting Factors
#       VDX       VDY       VCX       VCY       VAN
1  0.000000  0.000000  0.000000  0.000000  0.000000
2  0.000000  0.000000  0.000000  0.000000  0.000000
3  0.000000  0.000000  0.000000  0.000000  0.000000

Wavelengths     : 1
Units: Microns
#           Value          Weight
 1        0.589000        1.000000
```

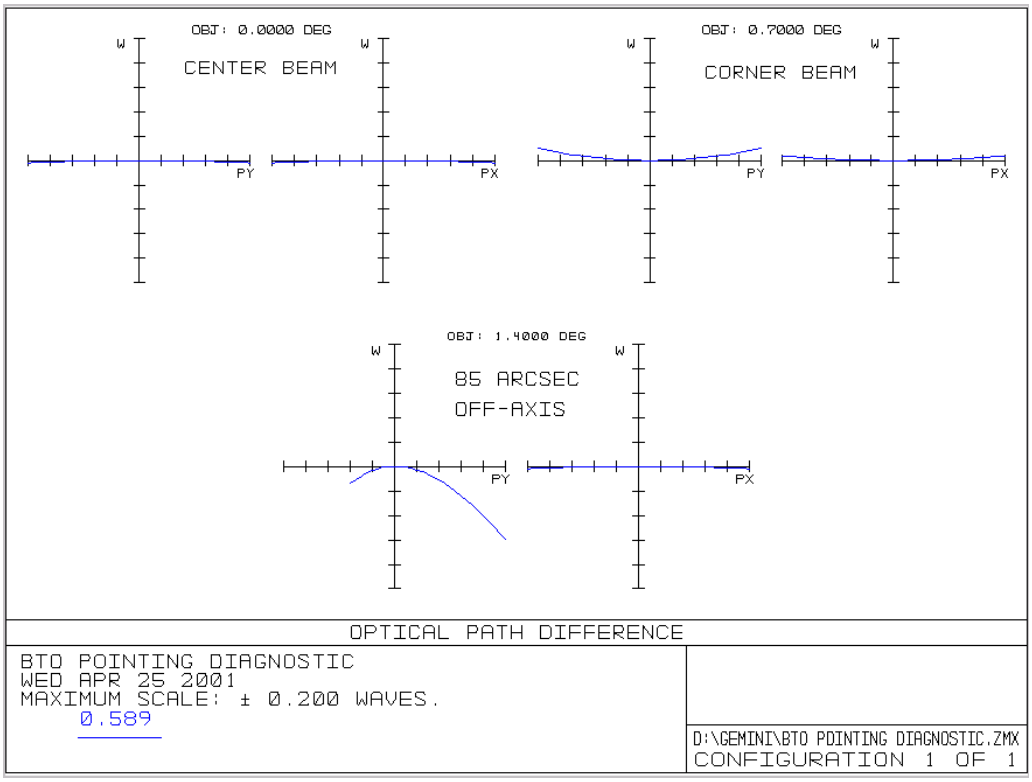

1.2.2. Centering diagnostic

The centering diagnostics are designed as an afocal telescope which relay a desired plane in object space to a diagnostic CCD. There has been some discussion as to what plane is the best one to re-image onto the CCD. The two obvious choices are the LLT pupil plane and the FSA/M plane. If the centering diagnostic images the LLT plane, then the centering camera will show the 5 beams overlaying each other when properly aligned. This sounds like a desirable characteristic, but the task is also done by the camera looking down on the LLT primary, albeit somewhat more crudely. In fact, the LLT camera has somewhat more information since it can also see the edges of the exit pupil of the system, whereas the centering camera can only see relative registration of the beams.

If the centering diagnostic images the FSA/M plane onto the CCD, then we have an indicator of whether the beams are in the correct positions with respect to the secondary vane. This, too, is a useful characteristic, although its function is somewhat performed by alignment cameras looking at the FSA/M.

In either case, the closed-loop function of the diagnostics is to keep the beams on the proper paths into the LLT. Since controlling to any point plus an angle on the beam path yields the same well-aligned result, it doesn't really matter which configuration is chosen. The only difference is in the ancillary alignment/troubleshooting capabilities that the choice of imaged plane yields.

A design which images the LLT pupil plane to the CCD is given here. The relay could be done with a simple positive lens, but the result would not be telecentric in image space with respect to the collimated beam; a change in focus would yield a change in size of the image, which could be misleading in diagnosing a problem.

As with the pointing diagnostic, the candidate CCD is a Cooke Corp. Pixelfly SVGA (1280x1024, 6.7 micron square pixels). The beam size into the camera is approximately 50% of the short side of the detector to allow for misalignment.

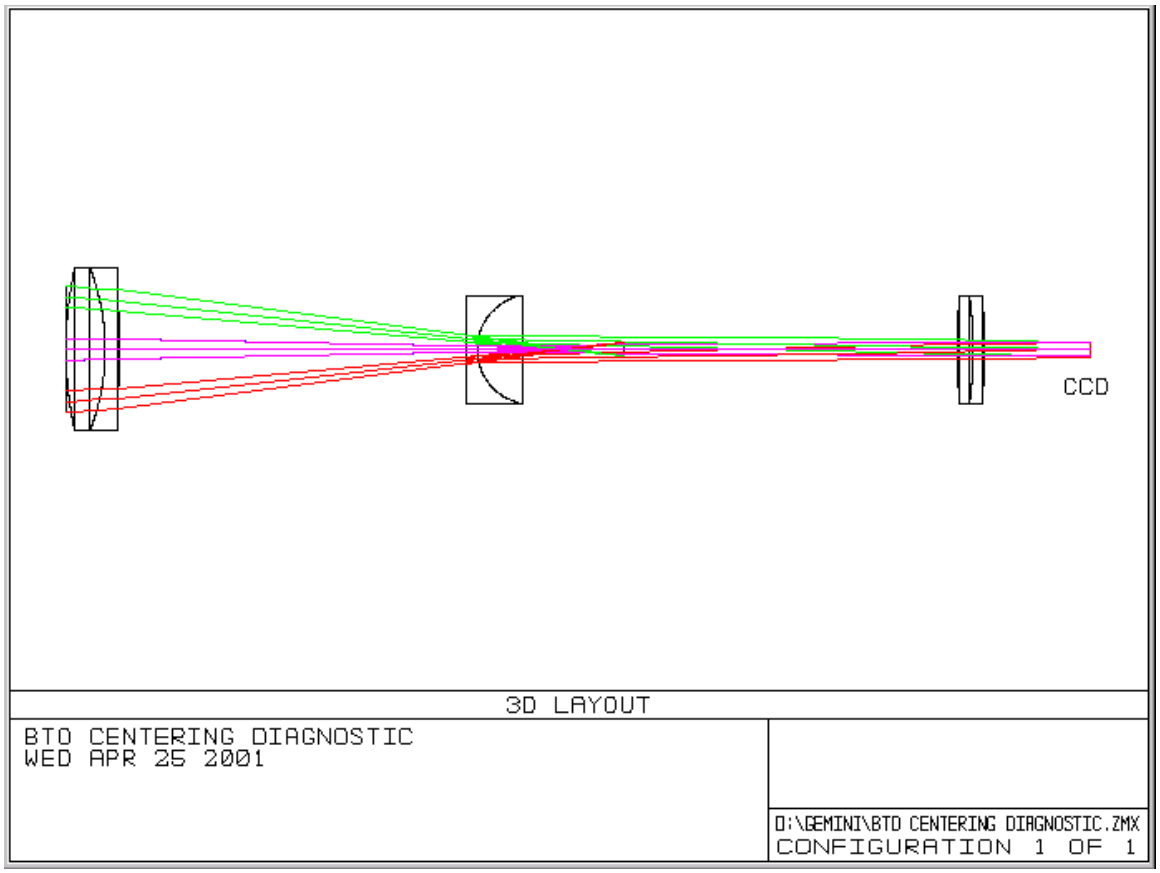

	Surf:Type	Comment	Radius	Thickness		Glass		Semi-Diameter		Conic
OBJ	Standard		Infinity	Infinity				Infinity		0.000000
STO	Standard	LLT PUPIL	Infinity	-1000.000000				2.500000		0.000000
2	Standard		Infinity	0.000000				14.717913		0.000000
3*	Standard	PAC074	87.780000	9.200000		BAFN10		19.049999	U	0.000000
4*	Standard		-52.752000	3.200000		SF10		19.049999	U	0.000000
5*	Standard		-484.254000	118.250745	M			19.049999	U	0.000000
6	Standard		Infinity	-36.832000	V			1.552767		0.000000
7*	Standard		Infinity	2.500000		BK7		12.700000	U	0.000000
8*	Standard	KPC043	12.920000	112.365637	V			12.700000	U	0.000000
9*	Standard	PAC064	121.712000	3.800000		BK7		12.700000	U	0.000000
10*	Standard		-89.718000	2.500000		SF5		12.700000	U	0.000000
11*	Standard		-268.159000	25.015618	V			12.700000	U	0.000000
IMA	Standard	CCD	Infinity					1.743680		0.000000

```
System/Prescription Data

File : D:\Gemini\BTO centering diagnostic.ZMX
Title: BTO centering diagnostic
Date : WED APR 25 2001

LENS NOTES:

       images LLT pupil to CCD



GENERAL LENS DATA:

Surfaces                 :               12
Stop                     :                1
System Aperture          : Entrance Pupil Diameter = 5
Glass Catalogs           : Schott
Ray Aiming               : Off
Apodization              :Uniform, factor =   0.00000E+000
Effective Focal Length   :         -532666 (in air)
Effective Focal Length   :         -532666 (in image space)
Back Focal Length        :       -346797.4
Total Track              :            1000
Image Space F/#          :        106533.2
Paraxial Working F/#     :           10000
Working F/#              :           10000
Image Space NA           :   4.693369e-006
Object Space NA          :         2.5e-010
Stop Radius              :             2.5
Paraxial Image Height    :        6508.067
Paraxial Magnification   :               0
Entrance Pupil Diameter  :               5
Entrance Pupil Position  :               0
Exit Pupil Diameter      :        3.255513
Exit Pupil Position      :       -2.233061
Field Type               : Angle in degrees
Maximum Field            :             0.7
Primary Wave             :           0.589
Lens Units               :   Millimeters
Angular Magnification    :        1.535856

Fields          : 5
Field Type: Angle in degrees
#         X-Value         Y-Value          Weight
 1        0.000000        0.000000        1.000000
 2        0.000000       -0.700000        1.000000
 3        0.000000        0.700000        1.000000
 4       -0.700000        0.000000        1.000000
 5        0.700000        0.000000        1.000000

Vignetting Factors
#        VDX       VDY       VCX       VCY       VAN
1  0.000000  0.000000  0.000000  0.000000  0.000000
2  0.000000  0.000000  0.000000  0.000000  0.000000
3  0.000000  0.000000  0.000000  0.000000  0.000000
4  0.000000  0.000000  0.000000  0.000000  0.000000
5  0.000000  0.000000  0.000000  0.000000  0.000000

Wavelengths     : 1
Units: Microns
#           Value          Weight
 1        0.589000        1.000000
```

1.3. XSM design and fast t/t array (FSA/M) design

The XSM consists of 5 separate 12.7mm diameter mirrors, arranged in an X-pattern. The XSM is the first place in the BTO where the beams form the X constellation pattern that will be seen on the sky. In general, the mirrors of the XSM are arranged at different angles since the beams will be coming at different beam heights off of the table. The exact arrangement of the t/t mirrors and the adjacent array of mirrors was a consideration in the CoDR, and the resulting clever design (involving evenly-spaced, vertically-arranged beams which then are intercepted by staggered mirrors in order to achieve an X-pattern), with some modifications, is an option for the final design. However, the drivers for this solution have been obviated by the lack of available small (<15mm diameter) fast t/t stages and the change in configuration that has brought two (rather than one in the CoDR) closed-loop arrays before the XSM

position. Designers may consider, then, any approach that delivers the beams to the XSM in the right places (in the X pattern) within the one-time, manual tilt adjustment range of the XSM mirror mounts. This would include a solution where the FSA mirrors are arranged unstaggered, vertically above one another; a 27mm center-to-center separation between mirrors is feasible.

The sketch below shows one feasible approach for the detailed design of the XSM. The main difficulty in the XSM design is interference between the center mirror mount and the corner mirror mounts. Displacing the center mirror mount towards the rear of the assembly and bringing the mirror in an adapter cell to the plane of the other mirrors resolves the interference.

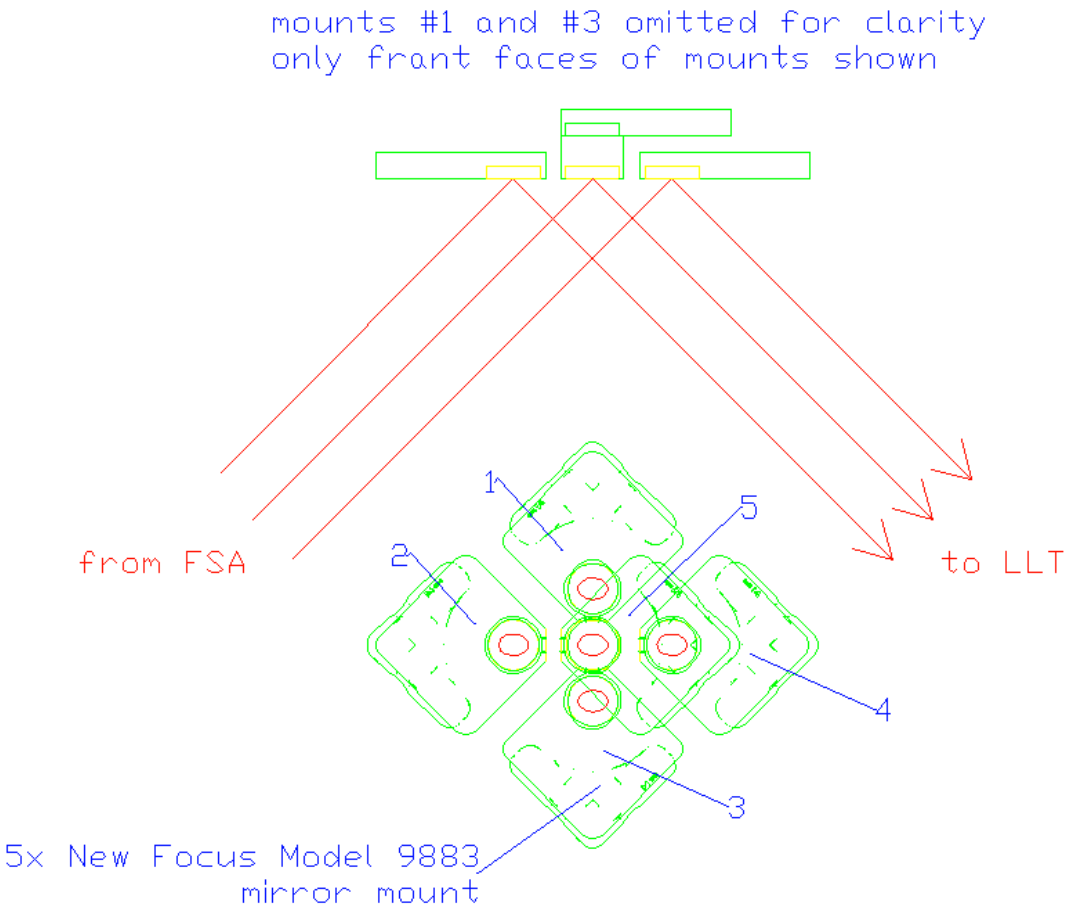

1.4. K-mirror design

The K-mirror is a 3-mirror configuration that rotates about an axis parallel to the incoming beam; this rotates the constellation. The K-mirror is controlled via a look-up table that is keyed to the orientation of the main telescope. An initial design is given below, with ZEMAX prescription and relevant figures. The path length through the K mirror is somewhat longer than the "straight-through" path length; the path length difference in this design is 17.9mm.

The rotation of the k-mirror needs to be done with a motorized open-aperture rotation stage, such as the New Focus 8401. The fixture should be one-time adjustable in x and y so that the central beam can be centered on the rotation axis of the stage; this will avoid pupil wander as the K mirror rotates.

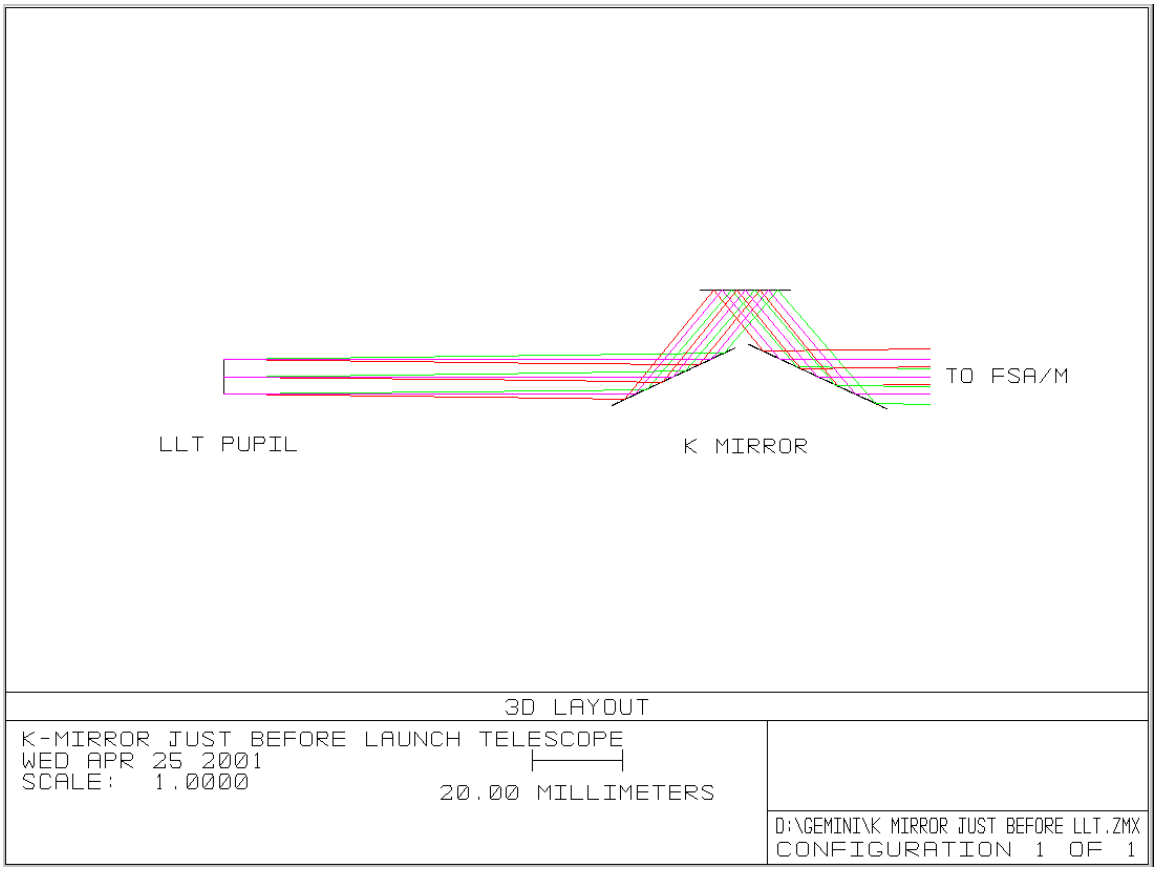

Surf:Type		Comment	Radius	Thickness	Glass		Semi-Diameter		Conic	Par 0(unused)	Decenter X	Decenter Y	Tilt About X	
OBJ	Standard		Infinity	Infinity			Infinity		0.000000					
STO	Standard	APPROX LLT PU..	Infinity	75.000000			3.950000		0.000000					
2	Standard	GOING BACKWARDS	Infinity	25.000000			4.866343		0.000000					
3	Coord Break			0.000000	-		0.000000				0.000000	0.000000	65.000000	
4*	Standard	K MIRROR #1	Infinity	0.000000	MIRROR		15.000000	U	0.000000					
5	Coord Break			-25.000000	-		0.000000				0.000000	0.000000	65.000000	P
6	Coord Break			0.000000	-		0.000000				0.000000	0.000000	-40.000000	P
7*	Standard	K MIRROR #2	Infinity	0.000000	MIRROR		10.000000	U	0.000000					
8	Coord Break			25.000000	P -		0.000000				0.000000	0.000000	-40.000000	P
9	Coord Break			0.000000	-		0.000000				0.000000	0.000000	65.000000	P
10*	Standard	K MIRROR #3	Infinity	0.000000	MIRROR		17.000000	U	0.000000					
11	Coord Break			-25.000000	-		0.000000				0.000000	0.000000	65.000000	P
IMA	Standard		Infinity				6.088135		0.000000					

```
System/Prescription Data

File : D:\Gemini\k mirror just before LLT.ZMX
Title: K-mirror just before launch telescope
Date : WED APR 25 2001

LENS NOTES:

       Prescription follows beam backwards starting at LLT entrance pupil
       Beam size corresponds to 99% encircled energy diameter


GENERAL LENS DATA:

Surfaces                 :               12
Stop                     :                1
System Aperture          : Entrance Pupil Diameter = 7.9
Glass Catalogs           : Schott
Ray Aiming               : Off
Apodization              :Uniform, factor =   0.00000E+000
Effective Focal Length   :         -1e+010 (in air)
Effective Focal Length   :         -1e+010 (in image space)
Total Track              :             100
Image Space F/#          :   1.265823e+009
Paraxial Working F/#     :           10000
Working F/#              :           10000
Image Space NA           :               0
Object Space NA          :       3.95e-010
Stop Radius              :            3.95
Paraxial Image Height    :        2.138135
Paraxial Magnification   :               0
Entrance Pupil Diameter  :             7.9
Entrance Pupil Position  :               0
Exit Pupil Diameter      :             7.9
Exit Pupil Position      :             175
Field Type               : Angle in degrees
Maximum Field            :             0.7
Primary Wave             :          0.5896
Lens Units               :   Millimeters
Angular Magnification    :              -1

Fields          : 5
Field Type: Angle in degrees
#         X-Value         Y-Value          Weight
 1       0.000000        0.000000        1.000000
 2       0.000000        0.700000        1.000000
 3       0.000000       -0.700000        1.000000
 4       0.700000        0.000000        1.000000
 5      -0.700000        0.000000        1.000000

Vignetting Factors
#        VDX        VDY        VCX        VCY        VAN
1  0.000000   0.000000   0.000000   0.000000   0.000000
2  0.000000   0.000000   0.000000   0.000000   0.000000
3  0.000000   0.000000   0.000000   0.000000   0.000000
4  0.000000   0.000000   0.000000   0.000000   0.000000
5  0.000000   0.000000   0.000000   0.000000   0.000000

Wavelengths     : 1
Units: Microns
#           Value          Weight
 1       0.589600        1.000000
```

2. Alignment procedure

The following sections give a detailed explanation of the error budget presented in Table 1 below.

2.1. Stages of alignment

Alignment through the beam transfer optics train is accomplished in four stages:

1) Mount placement to capture range of motorized adjustment: The mirror mounts must be installed so that the motorized adjustment ranges include the nominally aligned position.

2) Remote alignment and P&C capture: Motorized adjustment must be accurate enough that the beams enter the capture range of diagnostic sensors for handoff to low-bandwidth pointing and centering (P&C) control. The motorized adjustment range for the pointing and centering mirrors on the BTO table must allow for open-loop compensation of flexure of the LLT as a function of zenith angle.

3) P&C closed loop: The pointing control system must control the beams to within the capture range of the fast tip/tilt sensors in the AO system. The centering control system must keep the beam aligned to the LLT entrance pupil..

4) High speed closed loop tip/tilt control: the high-speed tip/tilt mirror must have sufficient range to cover tip/tilt excursions introduced by the atmosphere and be controlled accurately enough to achieve the on-sky pointing requirement.

Separate error budgets are developed for each stage.

2.2. Requirements

The BTO design for the 5-beam system must be compatible with a single beam LGS system (CoDR p.74). The on-sky pointing accuracy requirement is 0.05 arcseconds rms for each of the 5 beams in a nominal star pattern (CoDR Table 24, p.75). The capture range of the AO fast tip/tilt sensor is 1 arcsecond on the sky (CoDR 5.1.2.2, p.63).

The laser beams must “overlap fully” on the LLT primary, according to CoDR appendix H, sec 2.3, p.5. We interpret this (arbitrarily) to mean that the beam to beam overlap at the LLT entrance pupil must be less than 10% of the beam diameter (0.5 mm) and that the beams must be centered on the LLT entrance pupil to within 0.5 mm of the LLT input optical axis. Aberration analysis of the LLT design should be performed to determine if this is sufficient, or overly strict, for attaining the required output wavefront quality. A 10% shift of the beam on the LLT primary corresponds to 30 mm motion. The beam is 300 mm 1/e2 diameter and the LLT primary clear aperture is 450 mm (CoDR Appendix I, p.8; LLT Specifications and Requirements Document, 2.4.4, p.12).

Gemini Laser Beam Transfer Optics
Pointing Tolerance and Dynamic Range Budget

Don Gavel, LLNL 3/29/01

Flex of top end position	2	mm	17.4532925 mr/degree
Flex of top end angle	30	arcsec	0.00484814 mr/arcsec
LLT magnification	60	x	
LGS separation	42.5	arcsec	
Beam size	5	mm	
Max seeing	3	arcsec	

Stage 1: Mount Alignment

From*	To	dist., m	mirror size, mm	mounting tolerance angle, mr	beam position error at end of path (to-mirror), mm	path
Laser	Centering array			17.4532925		
Centering array	Pointing array	1		17.4532925		
Pointing array	Primary ring fold mirror	0		17.4532925		
Primary ring fold mirror	Top-end ring mirror	12		17.4532925	209.4395102	up the side of the telescope
Top-end ring mirror	Fast steering mirrors	3.5		17.4532925	61.08652382	along the spider vane
Fast steering mirrors	X shaping mirror	0.4	25	17.4532925	6.981317008	
X shaping mirror	Centering mirror	1		17.4532925	17.45329252	
Centering mirror	Pointing mirror	0.25		17.4532925	4.36332313	
Pointing mirror	LLT pupil	0.15		17.4532925	2.617993878	into LLT virtual pupil
LLT pupil	sky					

*spreadsheet entry values apply to the "from" mirror, unless otherwise indicated

Stage 2: Remote Alignment for P&C Capture, and remove elevation-dependent flexure open-loop

From*	To	dist., m	mirror size, mm	anticipated flexure sag along path, mm	anticipated flexure angle, mr	motorized dynamic range required, mr	beam position error at end of path (to-mirror), mm	pointing error budget, mr	path
Laser	Centering array								
Centering array (CA)	Pointing array	1				25			
Pointing array (PA)	Primary ring fold mirror	0	25						primary fold and pointing array ar
Primary ring fold mirror	Top-end ring mirror	12	25	2	0.1454441	27.395444	0.5		up the side of the telescope
Top-end ring mirror	Fast steering mirrors	3.5			0	17.453293	0.5	2.083333	along the spider vane
Fast steering mirrors	X shaping mirror	0.4	25				0.5	2.5	
X shaping mirror	Diagnostic pupil	1.4	10			17.453293	1.5	2	
Diagnostic pupil								4.3	mm on the pupil
Diagnostic far-field								79.37549	arcsec on the sky
X shaping mirror	Centering mirror	1							
Centering mirror	Pointing mirror	0.25				22.68928			
Pointing mirror	LLT pupil	0.15	11.58862			31.415927	0.5		into LLT virtual pupil
LLT pupil	sky								

Stage 3: Closed loop P&C, and align optics downstream of P&C using backpropagating star

From*	To	dist., m	anticipated flexure sag along path, mm	anticipated flexure angle, mr	motorized dynamic range required, mr	beam position error at end of path (to-mirror), mm	pointing error budget, mr	path
Laser	Centering array							
Centering array	Pointing array						0.205689	
Pointing array	Primary ring fold mirror						0.205689	
Primary ring fold mirror	Top-end ring mirror	12		2	27.395444	0.5		up the side of the telescope
Top-end ring mirror	Fast steering mirrors	3.5		0	17.453293	0.5		along the spider vane
Fast steering mirrors	X shaping mirror	0.4				0.5		
X shaping mirror	Diagnostic pupil	1.4				0.5		
Diagnostic near-field sensor						0.5		
Diagnostic far-field sensor							0.408248	arcsec on the sky
X shaping mirror	Centering mirror	1						
Centering mirror	Pointing mirror	0.25			22.68928		0.118755	mr
K mirror							0.118755	mr
Pointing mirror	LLT pupil	0.15			31.415927	0.5	0.118755	mr
LLT pupil	LLT secondary							
LLT secondary	LLT primary						0.118755	mr
LLT primary	sky						0.001979	mr
							1	arcsec on the sky to acquire

These terms RSS to uplink tip/tilt acquisition requirement

6 terms

Stage 4: Closed loop Fast Steering

From*	To	dist., m	dynamic range required, mr	pointing error budget	
Laser	Centering array				
Centering array	Pointing array				
Pointing array	Primary ring fold mirror				
Primary ring fold mirror	Top-end ring mirror	12			
Top-end ring mirror	Fast steering mirrors	3.5			
Fast steering mirrors	X shaping mirror	0.4	0.8726646	0.014544	
X shaping mirror	Diagnostic pupil	1.4			
Diagnostic near-field sensor					
High bandwidth uplink tip/tilt sensor (in AO system)				0.05	arcsec on the sky
X shaping mirror	Centering mirror	1			
Centering mirror	Pointing mirror	0.25			
Pointing mirror	LLT pupil	0.15			
LLT pupil	sky			0.05	arcsec on the sky pointing stability requireme

Table 1 BTO pointing tolerance and dynamic range budget

2.3. Beam transfer method

The beams exit the laser and are reflected off centering and pointing arrays. One purpose of these arrays is to statically configure the 5 beams for transfer across the telescope primary but hidden behind one of the secondary support spider vanes. The 5 beams are stacked on top of one another so that their nominal beam width is within the width of the vane, thus shadowing air-scattered laser light from entering the AO system. Cameras located at the top-end ring mirror and at the fast tip/tilt mirrors sense these beam positions. The second purpose of the pointing and centering arrays is to dynamically compensate for the flexure of the top-end of the telescope, so that the beams remain centered across the spider vane as the telescope moves off zenith. The top-end is expected to sag 2 mm and rotate 30 arcseconds as the telescope is moved from zenith to horizon.

Once crossing over the vane, the beams hit the fast tip/tilt mirrors on the BTO table. The beams hit these mirrors nominally on center and, with the tip/tilt mirrors at center range, the beams reflected off these mirrors hit defined positions on the X-shaping mirror. Beams leaving the X-shaping mirror are in the 5-beam configuration for the sky and are converging at an angle so that they overlap at the pupil of the LLT and are projected on the sky by the LLT so they form the defined pattern (CoDR Fig 33, p.82).

A pair of pointing and centering mirrors directs the beam into the LLT. In their alignment role, these mirrors bring the beam on to the input centerline of the LLT. They also function to offload the fast tip/tilt mirrors to keep the laser beacons fixed in the sky with respect to the AO axis, compensating the long-term flexure of the LLT axis with elevation.

2.4. Explanation of Error Budget

Note: in the discussion below, the doubling of beam angles due to the reflection off mirror surfaces has been neglected. The numbers indicate beam angle deviations with respect to nominal. Although actual mirror angular motion might generally be half this, the exact motion of the mirror will depend on the geometry of the mount gimbals. We will ignore this whole issue with the statement that the dynamic range requirements on mounts will be no more than the numbers indicated and the motorized mount angle accuracy requirements will be no less than half the indicated numbers.

2.4.1. Stage 1: Mount placement to capture range of motorized adjustment

Mounts will be manually positioned to the accuracy needed for subsequent adjustment by motors and/or micrometers. The usual accuracy of manual positioning is on the order of one degree (17.45 mr). In the spreadsheet, the resulting beam positioning error is calculated as this one degree angle times the distance between mirror points.

2.4.2. Stage 2: Remote alignment and P&C capture

The remote alignment must establish the beam line across the top-end vane, be within the control range of the pointing and centering arrays, and within the field of view of the pointing and centering diagnostic sensors.

2.4.2.1. Range of the pointing and centering array mirrors

Proceeding from top to bottom in the Stage 2 error and dynamic range budget, we see that the primary fold mirror (we assume this is the same as the pointing array) must be able to take up top-end sag and rotation, as well as the initial mounting accuracy of the top-end fold mirror. The 0.5 mm initial positioning accuracy at the top-end fold mirror is achieved with a camera looking at the scattered light from this mirror. Another camera looks at the tip/tilt array at the "receiving" end to assure similar positioning accuracy there. Now, imagine a beam propagating backwards through these two fixed points in space, reflecting off the top-end fold mirror and going down to the pointing array. If the top-end fold mirror is pointed to an accuracy of 2mr, the beam reaches the pointing array within 25 mm of center. Therefore the pointing array mirrors must be >25 mm diameter, and the centering array must steer the forward-propagating laser beam by 25 mr (assuming a 1 meter distance between pointing and centering arrays) so that it hits this point on the pointing array mirror. Because of the 25 mr steering from centering array to pointing array, the beam angle as it hits the pointing array mirror (propagating forward) is in error, so the pointing array mirror must tilt 25 mr to compensate for it. Add to this add the 2 mr beam angle necessary to go up the telescope and hit the proper position on the top-end fold mirror. Now, the gravity-induced sag of the top-end by 2 mm and the tilt of the top end of 30 arcsec (0.15 mr) must also be taken up by the pointing array mirror. These flexure terms total to 0.31 mr. The total range of the pointing array is 29 mr. The total range of the centering array is 25 mr.

2.4.2.2. Top-end ring fold mirror range and accuracy

The mirror at the top-end ring must have a range to cover its own mounting accuracy of 1 degree (17 mr). The accuracy is determined by the ability to point to some point on the pointing array mirror, an area we arbitrarily set to 25 mm, which, over the 12 meter path amounts to 2 mr pointing accuracy.

2.4.2.3. Fast steering array range and accuracy

The fast steering array assembly is not motorized. However, we will assume that during initial alignment it can be tapped into place to position the beam on the X-shaping mirror to within 1 mm. This is 2.5 mr pointing accuracy.

2.4.2.4. X-shaping mirror size, range, and accuracy

We allow for 0.5 mm random positioning of the beam on the fast steering array plus the 1 mm initial alignment accuracy to arrive at a requirement that each receiving mirror in the X-shaping array be larger than 1.5 mm. The X-shaping array will be remotely adjustable

to a range of 1 degree (17 mr) to take up initial mounting accuracy. We allow 2 mr pointing accuracy.

2.4.2.5. Diagnostic sensor range

The pointing and centering diagnostic sensors must have fields of view to cover the accumulated inaccuracies of the upstream optics after initial alignment. The alignment brings the beam to a position accuracy of 1.5 mm and an angular accuracy of 2 mr at the X-shaping mirror. Computing the pupil shift after a path length of 1.4 m to the LLT virtual pupil gives 4.3 mm, approximately one beam width.

In order to view the entire 5 beam constellation after initial alignment, the pointing camera must have a field of view (on the sky) of 42 arcseconds constellation size plus the 30 arcsecond flexure of the top-end plus the 2 mr / 60 = 7 arcsecond alignment accuracy of the X-shaping mirror, totaling 79 arcseconds on the sky.

2.4.2.6. Pointing and Centering mirror range and accuracy

The pointing and centering mirrors on the BTO table are used to compensate for the overall shift of the beam constellation on the sky resulting from flexure of the top-end as a function of zenith angle. They are aligned initially by looking at a star through the LLT and adjusting to put the star in the proper position on the pointing and centering diagnostic sensors (a retro-mirror scheme allows backward-propagating starlight to enter the diagnostic package). The pointing range must be enough to take up the anticipated flexure, 30 arcseconds on the sky (9 mr on the BTO table), while the centering must keep the beam on the LLT entrance pupil. The pointing (P) and centering (C) mirrors are not purely "pointing" and "centering", but are cross-coupled, so they each take up some of the job of pointing. The P mirror (actually 150 mm from the LLT pupil) must point the beam the 30 arcseconds times the 60x magnification ratio and also undo the angle introduced by the C mirror which recentered the pupil. The resuting motions are:

$$\theta_C = \theta_{flexure} \times M \times (Z_{pupil\text{-}P})/(Z_{P\text{-}C})$$

$$\theta_P = \theta_{flexure} \times M + \theta_C$$

where $\theta_{flexure}$ is 30 arcseconds, M is the LLT beam expansion ratio, $Z_{pupil\text{-}P}$ is the distance from P mirror to the pupil (150 mm), and $Z_{P\text{-}C}$ is the distance from the C mirror to the P mirror (250 mm). We add to these the 1 degree mounting accuracy to get 23 mr range for the C mirror and 32 mr range for the P mirror.

The accuracy must be good enough to off-load the fast tip/tilt mirrors. The tip/tilt mirrors have an approximate 1 mr range, so 0.5 mr accuracy is appropriate for the pointing and centering mirrors.

2.4.3. Stage 3: P&C closed loop

The closed loop P&C system must provide enough accuracy that the AO system's wavefront sensors can acquire the guide stars. We set a somewhat conservative limit of 1 arcsecond on the sky as the necessary accuracy.

2.4.3.1. Accuracy of the pointing and centering arrays

The pointing and centering arrays must position each beam separately to 1 arcsecond. This is 1 × M / sqrt(2) = 0.2 mr for each mirror element (the sqrt(2) factor distributes the error evenly between pointing and centering elements).

2.4.3.2. Accuracy of the diagnostic sensor and stability of downstream optics

We distribute the 1 arcsecond error budget evenly over 6 sources of pointing error: the P&C diagnostic sensor and 5 "optics" downstream of the diagnostic split (C mirror, K mirror, P mirror, LLT secondary, LLT primary). To achieve 1 arcsecond accuracy, these optics must be stable against vibration and other drift sources to 1 arcsecond × M / sqrt(6) = 0.12 mr. The diagnostic pointing sensor must be accurate to 1 arcsecond / sqrt(6) = 0.41 arcsecond.

2.4.4. Stage 4: High bandwidth closed loop tip/tilt control

Once the beams are acquired into the wavefront sensors, the high-bandwidth tip/tilt loop takes over. This loop is specified (CoDR p.75) at 0.05 arcseconds accuracy. The fast tip/tilt mirrors must have a resolution of 0.05 arcsecond × M = 15 μr to achieve this.

3. Rayleigh backscatter from the beams behind the secondary spider vane

On their way to the BTOOB and LLT behind the telescope secondary, the 5 laser beams must traverse across the telescope aperture in front of the primary mirror. In order to minimize the Rayleigh scatter into the AO wavefront sensors, these beams are hidden behind one of the secondary support "spider" vanes. This section presents an analysis of how much Rayleigh scattered light from these beams will enter the AO wavefront sensor field of view.

The beams are stacked vertically and centered behind the 10 mm wide vane. The beams have a Gaussian intensity profile, with $1/e^2$ diameter of 5 mm. The geometry is depicted in the figure below.

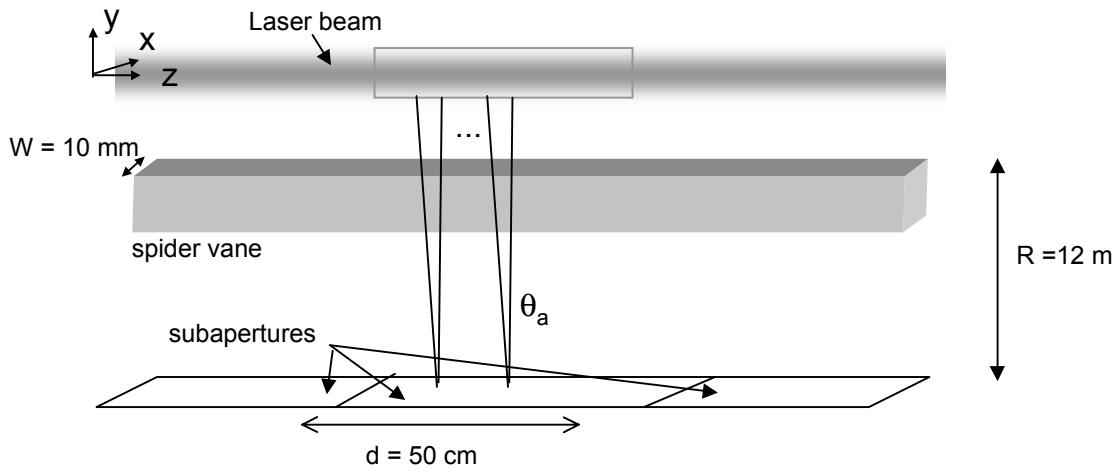

Figure 1 - Rayleigh light from beams behind the vane scattering into wavefront sensor subapertures

In the absence of the spider vane, each subaperture would see a section of the beam 50 cm long (the "diameter" of the subaperture), but only photons entering within the acceptance angle θ_a will hit one of the quad cell pixels. The wavefront sensor platescale is one arcsecond per pixel so the acceptance angle is 2 arcseconds for a 2x2 quadcell. The acceptance angle adds an additional $R\theta_a = 58$ microns on each end along the z axis, negligible compared to the 50 cm subaperture size. With the beam exactly centered behind the spider vane, the light coming from the Gaussian tails of the beam (along the x axis) is within the acceptance angle (see Figure 2 below).

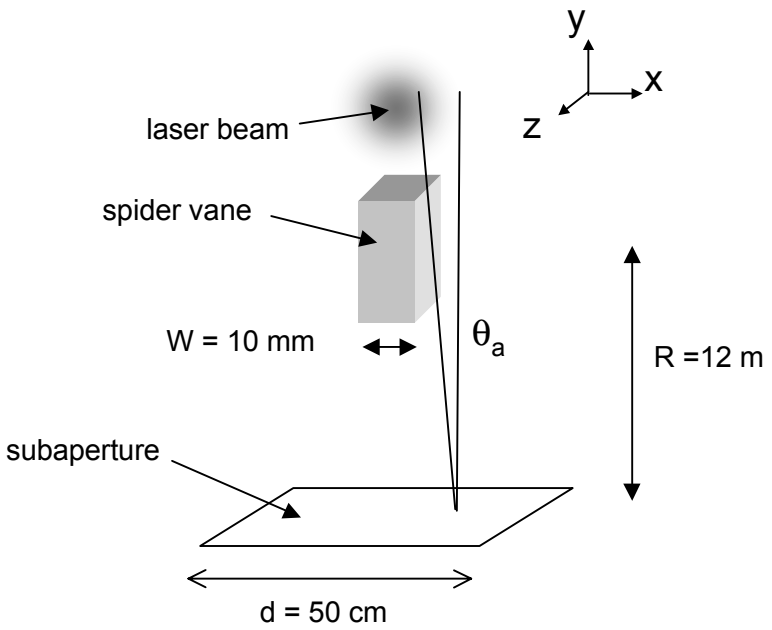

Figure 2 - End-on view of Rayleigh light from beams behind the vane scattering into a subaperture

If the beam is not baffled on the sides we must assume that all the light from the Gaussian tails enters the wavefront sensor, according to the geometry of Figure 2. The total scatter depends on the atmospheric scattering coefficient, K_s, which is the percentage of incident light volume-scattered per unit propagation length. Scattering coefficient consists of both Rayleigh (molecular scattering) and aerosol terms. The molecular scattering coefficient at the 3.5 km Cerro Pachon altitude is less than 8 x 10^{-6} (Infrared Handbook, 1978 edition, Table 4-4). The aerosol scattering varies considerably depending on the local conditions. Rural environments with 50 km visibility conditions can have an aerosol scattering coefficent as large as 10^{-4}. Along a 50 cm path, this amounts to 2.5 mw = 7.4 x 10^{15} photons/second volume-scattered light. The fraction of this light that is in the 2σ tails is about 0.0455 (w/2 = 5 mm is 2σ away from the center of the $1/e^2$ = 5 mm beam profile). The fraction of this light intercepted by the wavefront sensor's acceptance solid angle is $\theta_a^2/(4\ \pi)$ = 7.4 x 10^{-12}. Multiplying these factors together yields 2522 photons/second. For the typical AO frame rate of 100 Hz, this amounts to 25.2 photons per frame per subaperture. This will appear more or less uniformly over the 4 pixels, giving about 6.3 background photons per pixel, or, after background subtraction, approximately 2.5 additional Poisson noise photons. We emphasize that this is probably overestimated since the assumed scattering coefficient is conservatively large. However, it is recommended that the beam be baffled on the sides. This will cut off the Gaussian tail and also prevent atmospherically-scattered photons reflecting off the sides of the vain into the acceptance cone of the subaperture.

We provide the radiometric equation here for reference:

$$n_{ph} = 2T \int_{5\,\mathrm{mm}}^{25\,\mathrm{cm}} \int_{0}^{d} \frac{P}{h\upsilon} \cdot \frac{\theta_a^2}{4\pi} \cdot K_s dz \cdot \frac{1}{\sqrt{2\pi}\sigma} e^{-\frac{1}{2}(x/\sigma)^2} dx$$

where

n_{ph} = number of photons/subaperture/frame
P = laser power = 50 Watts
K_s = scattering coefficient = 10^{-4}
θ_a = acceptance angle = 2 arcsec
h = Plank's constant
ν = frequency of the laser light = 5.1 x 10^{14}
σ = Gaussian 1/e width of the laser beam profile = 1.8 mm
T = wavefront sensor sample interval = 10 ms
d = subaperture size = 50 cm

4. Rayleigh background light in the AO wavefront sensors

One of the possible laser scenarios is the use of continuous-wave lasers. In this case, the Rayleigh light from other beams in the 5-beam pattern can overlap with guidestar return on some subapertures. A "sky's eye" view of the Gemini MCAO laser geometry is shown in figure 3. We number the guidestars 0,1,2,3, and 4 corresponding to the central and 4 corner guidestars in the 5-beam pattern. The potential for interference is evident. For example, Rayleigh from guidestar 2 intersects the view of guidestar 0 from subapertures located along a diagonal x = y, x>0.

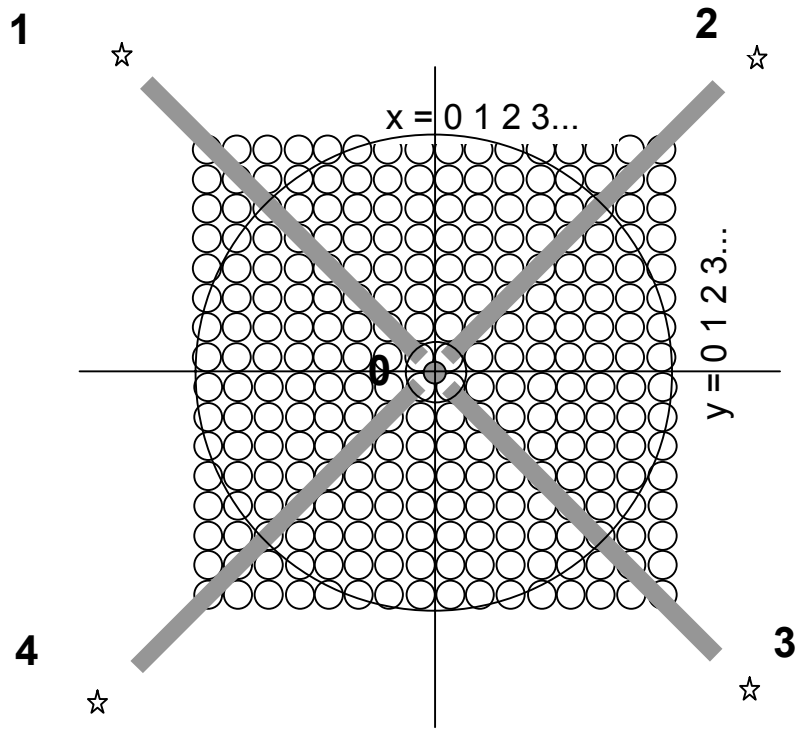

Figure 3 – MCAO laser geometry as seen from the sky, looking down on the Gemini telescope aperture.

We have simulated the Rayleigh backscatter and its imaging onto the wavefront sensor using a wave-optic simulation code. This code "launches" the laser light from behind the secondary and propagates it to the 5 guidestar positions. At each height long the way, the

propagating beam is imaged back into the wavefront sensor at a position in the focal plane that corresponds to the field angle of the beam at that altitude. The amount of backscattered light is computed according to a Rayleigh-backscatter coefficient vs altitude model.
The lidar equation gives the backscattered return at each altitude:

$$n_p = \left(\frac{P}{h\nu}\right)\sigma_B^R n_r(z)\left(\frac{d^2}{4\pi z^2}\right)\Delta z$$

where

n_p = number of backscattered photons
P = laser power
$\sigma_B^R n_r(z)$ = the backscatter coefficient (see below)
d = diameter of subaperture
z = altitude of scatter
The backscatter coefficient is calculated from a model developed by Gardner [C. S. Gardner, B. M. Welsh, and L. A. Thompson, Design and Performance Analysis of Adaptive Optical Telescopes Using Laser Guide Stars, Proc. IEEE, 78, 1990]:

$$\sigma_B^R n_R(z) = 3.6\times10^{-31}\frac{P(z)}{T(z)}\lambda^{-4.0117}$$

where

$P(z)$ = atmospheric pressure at altitude z
$T(z)$ = temperature at altitude z
λ = wavelength = 0.589 μ
Graphs of these equations are shown below. A backscatter coefficient table in Hardy [J. W. Hardy, Adaptive Optics for Astronomical Telescopes, Oxford University Press, 1998, Table 9.4] is compared to the Gardner model (which is also stated in Hardy as equation 7.4).

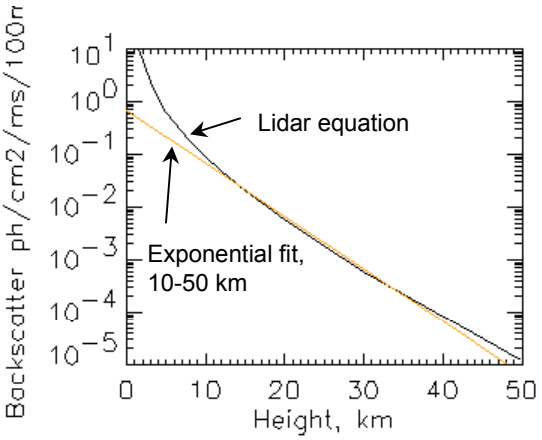

Figure 4a – Rayleigh return vs altitude

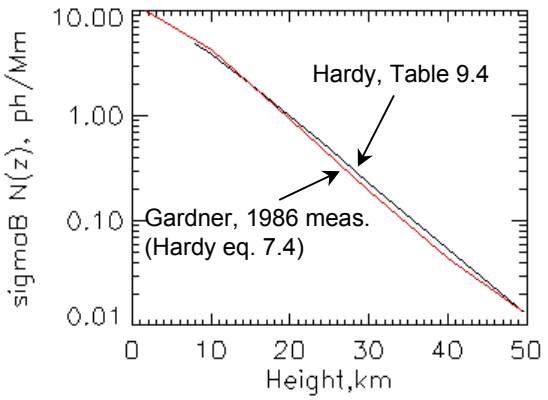

Figure 4b – Backscatter coefficient vs altitude

To validate these models we compared a simulation to real data from the laser guidestar system at Lick observatory (Figure 5).

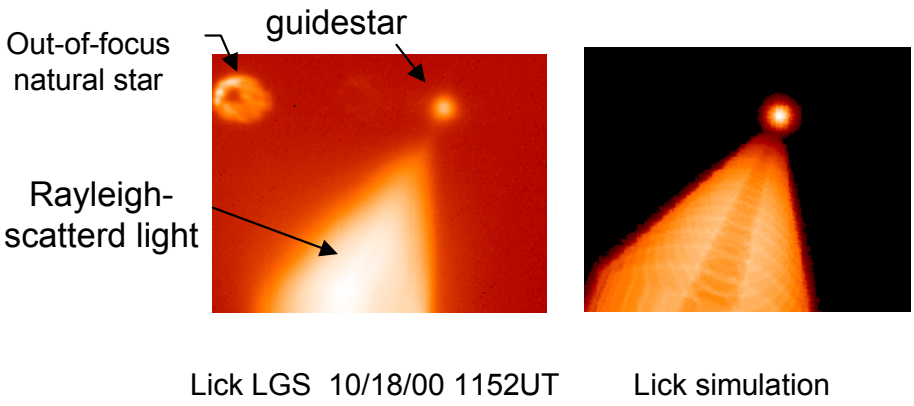

Figure 5 – Simulation (right) vs data (left) from the Lick observatory laser guidestar system. Field of view is approximately 48 arcseconds on a side

In the following set of figures, we show the predicted image-plane intensity distribution for a number of Gemini subapertures. These are on 16 x 16 arcsecond fields, with the guidestar in the center of the field (the guidestar itself is not shown except in the last picture). The subapertures and lasers are numbered according to the scheme in Figure 3. Integrated Rayleigh light in the 1 arcsecond wavefront sensor pixels is shown. A,B,C,D refer to the 4 pixels in the Hartmann quadcell. The total Rayleigh light per subaperture per frame can be computed from the numbers shown (units: photons/ms/cm^2) by multiplying by the subaperture area, 2500 cm^2 for a fully-illuminated subaperture, and the integration time (typically 10 ms). For comparison, the guidestar return is expected to be on the order of 0.3 photons/ms/cm^2. In some cases it can be seen that the Rayleigh background is as bright as the guidestar.

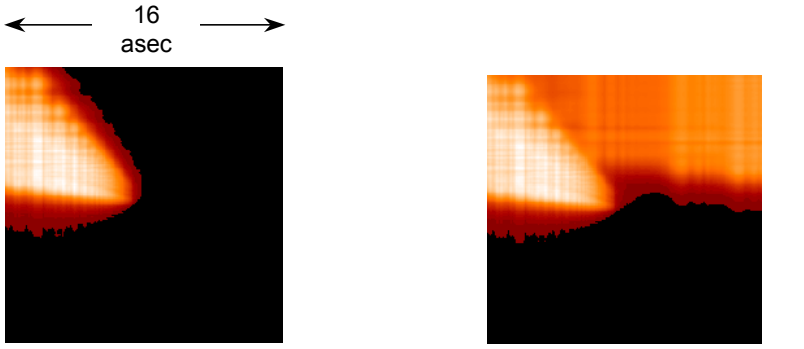

Subap [1,0], laser 0
(WFS on guidestar #0)

Subap [1,0], lasers 0 and 2

Rayleigh in the Hartmann quad-cell:

A=0.000444274 B=0.000109051

C=0.00369100 D=0.000967429

photons/ms/cm2/pixel

A=0.00103703 B=0.000704920

C=0.00477580 D=0.00205669

photons/ms/cm2/pixel

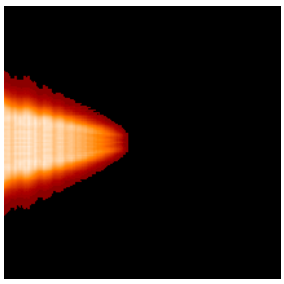

Subap [1,1], laser 0

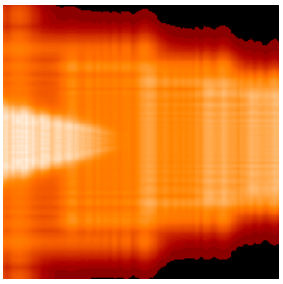

Subap [1,1], lasers 0 and 2

Rayleigh in the Hartmann quad-cell:

A=0.000684353 B=0.000333580

C=0.000680481 D=0.000329981

photons/ms/cm2/pixel

A=0.101302 B=0.150299

C=0.101351 D=0.150377

photons/ms/cm2/pixel

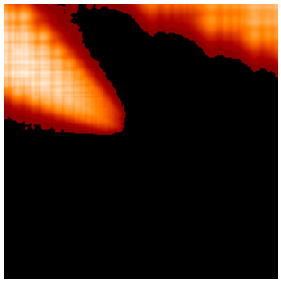

Subap [2,0], lasers 0 and 2

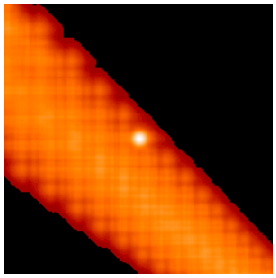

Subap [6,0], lasers 1 and 2,
(WFS for lgs 1)

Rayleigh in the Hartmann quad-cell:

A=4.07539e-006 B=2.14001e-006

C= 1.87567e-005 D=8.69122e-006

photons/ms/cm2/pixel

Rayleigh in the Hartmann quad-cell:

A=0.269123 B=0.0221941

C=0.264936 D=0.0221928

photons/ms/cm2/pixel

Figure 6 – Simulation results of Rayleigh backscatter into Gemini subapertures

The following figure shows pupil maps of the integrated Rayleigh backscatter in each subaperture. The figures show a 16 x 16 subaperture grid, overlayed on the circular Gemini aperture (4 subapertures in the middle are obscured by the secondary). The first map shows the Rayleigh backscatter into the wavefront sensor dedicated to looking at guidestar 0 (the center guidestar). This map is symmetric and shows the Rayleigh from the 4 corner lasers affecting subapertures mostly located along diagonals, that is, directly under the 4 laser beams. The second map shows the backscatter into the wavefront

sensor dedicated to looking at guidestar 1 (one of the corner guidestars). In this case, the interfering Rayleigh pattern is concentrated toward the other corner, generally opposite to the direction of the desired guidestar. The patterns for wavefront sensors 2,3, and 4 are exactly the same, only rotated at 90 degree increments accordingly. The data in this chart is available in digital form.

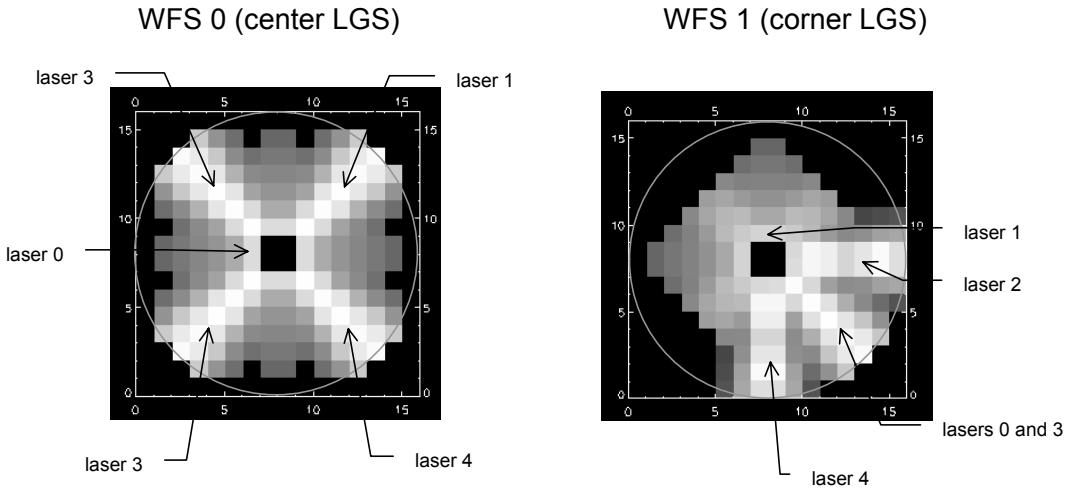

Figure 7 – Maps of integrated Rayleigh backscatter into the field of view of Hartmann subapertures. The map is a 16x16 grid of AO subapertures with grey-scale intensity indicatating the amount of Rayleigh backscatter in each subaperture. Laser beam "trails" from other lasers in the pattern are clearly visible. The associated laser's Rayleigh creates a circular pattern that is brightest on subapertures closest to the secondary.

5. Light scattered off of dust on BTO optics

Dust scattered light, while not of major importance to the goal of 0.8 throughput for the BTO optics, does contribute enough scattered light *power* to significantly effect the BTO heat dissipation budget. Unfortunately, predicting how much dust will be on a particular optic is very difficult. We can however make a rough estimate of dust scatter under assumptions of environment conditions. When more information about the dust environment of the Gemini dome(s) becomes available, we can compare to the assumptions made here.

According to [I. F., Stowers, Optical Cleanliness Specifications and Cleanliness Verification, SPIE 3782, 1999] "visibly dirty surfaces" contain greater than 10^3 particles per square mm of size greater than 10 microns. The dust size distribution on the optical surfaces will depend on the environment (particle distribution in the atmosphere), the orientation of the optic with respect to gravity, and the length of time the optic is exposed to the environment.
Measurements have shown that the dust size function generally fits a model given by

$$F(s) = 10^{\,0.926\,[\,\log_{10}{}^{2}(CL) - \log_{10}{}^{2}(s)\,]}$$

Where

F(s) = the number of particles larger than size s, per square foot

s = the particle diameter, in microns
CL = the "Cleanliness Level", defined as the particles size above which the cumulative particle count is 1 per square foot

"Visibly dirty" surfaces are stated as surfaces with cleanliness level 500 (one 500 micron particle/ft^2). "Clean" surfaces are at cleanliness level 50 (one 50 micron particle/ft^2). Note that the cumulative distribution model is valid only for s>1 since the function is not monotonically decreasing at smaller values of s.

We want to calculate the percentage area obscured by the dust particles. First, the number *density* function is calculated by taking the derivative of the cumulative function, $f(s) = -F'(s)$. This number density is then multiplied by the cross-sectional area $a = (\pi/4)\, s^2$ at each size bin s. Then the units are changed from "per square foot" to "per square micron" by multiplying by $1/(12 \times 2.54 \times 10^{-4})$. Finally, the density function is integrated to get the cumulative percent-area coverage

$$p(s_0) = \int_{s_0}^{\infty} -cF'(s)s^2\,ds$$

where $c = \pi/(4 \times 12 \times 2.54 \times 10^4)$, and s_0 is the minimum value of s (1 micron for this model). This function has been integrated numerically at various cleanliness levels:

Level	$p(s_0)$
1000	12%
500	0.3%
300	0.002%

6. Power dissipated in the fast tip/tilt stages

The tip/tilt stages located on the BTOOB are continually in operation at a high bandwidth in order to keep the laser beam nominally centered in the AO wavefront sensor quadcells. The question is: how much power is consumed by these stages? At first guess, one would think that energy loss due to hysteresis in the PZT actuators would be important. A quick calculation shows that this is quite negligible.

At any given Fourier frequency f, the atmosphere has a tilt power of

$$S_{tilt}(f) = 0.12\,(\lambda/D)^2\,(D/r_0)^2\,f_0^{-1/3}\,f^{2/3} \qquad \text{radians}^2/\text{Hz}$$

where f_0 is a characteristic frequency $f_0 = v/(\pi D)$, where v is the wind velocity and D is the beam diameter, and r_0 is Fried's seeing parameter. The motion of the tip/tilt mirror is M = 60 times this, since the beam is magnified by a factor of 60 by the LLT. The $f^{-2/3}$ atmospheric tilt spectrum is valid up to roughly the characteristic frequency f_0, above which the spectrum drops off rapidly [D. P. Greenwood and D. L. Fried, Power spectra requirements for wave-front-compensative systems, JOSA, 66, 1976]. The energy possessed by the tip/tilt mirror at frequency bin f is

$$E(f) = I\,\omega^2 = I\,(d\theta/dt)^2 = I\,(2\,\pi\,f)^2\,M^2\,S_{tilt}(f)$$

where I is the moment of inertia of the tip/tilt mirror (and the moving part of the tip/tilt stage it's glued to). The moment of inertial is roughly 5 g cm^2 for the 1 inch optic.
The hysteresis loss is given by

$$P_{loss}(f) = \eta\ f\ E(f)$$

where η is a hysteresis loss factor, typically 10% per cycle, and f is the number of cycles per second. Integrating this spectrum from f = 0 to f = f_0 gives

$$\int_0^{f_0} P_{loss}(f)df = \eta\ (6/5)\ (0.12)\ \ \pi^2\ M^2\ \ f_0^3\ \ r_0^{-2}\ I\ \lambda^2$$

Plugging in reasonable numbers for r_0 (20 cm) and wind velocity (20 m/sec), the total power loss is on the order of 10^{-12} Watts, certainly a negligible heat load!